OPEN ACCESS Freely available online

PLoS GENETICS

Reverse Genetic Analysis of the Yeast RSC Chromatin Remodeler Reveals a Role for RSC3 and SNF5 Homolog 1 in Ploidy Maintenance

Coen Campsteijn, Anne-Marie J. Wijnands-Collin, Colin Logie*

Molecular Biology Department, Nijmegen Centre for Molecular Life Sciences, Radboud University Nijmegen, Netherlands

The yeast "remodels the structure of chromatin" (RSC) complex is a multi-subunit "switching deficient/sucrose non-fermenting" type ATP-dependent nucleosome remodeler, with human counterparts that are well-established tumor suppressors. Using temperature-inducible degron fusions of all the essential RSC subunits, we set out to map RSC requirement as a function of the mitotic cell cycle. We found that RSC executes essential functions during G1, G2, and mitosis. Remarkably, we observed a doubling of chromosome complements when degron alleles of the RSC subunit *SFH1*, the yeast *hSNF5* tumor suppressor ortholog, and *RSC3* were combined. The requirement for simultaneous deregulation of *SFH1* and *RSC3* to induce these ploidy shifts was eliminated by knockout of the S-phase cyclin *CLB5* and by transient depletion of replication origin licensing factor Cdc6p. Further, combination of the degron alleles of *SFH1* and *RSC3*, with deletion alleles of each of the nine Cdc28/Cdk1-associated cyclins, revealed a strong and specific genetic interaction between the S-phase cyclin genes *CLB5* and *RSC3*, indicating a role for Rsc3p in proper S-phase regulation. Taken together, our results implicate RSC in regulation of the G1/S-phase transition and establish a hitherto unanticipated role for RSC-mediated chromatin remodeling in ploidy maintenance.

Citation: Campsteijn C, Wijnands-Collin AMJ, Logie C (2007) Reverse genetic analysis of the yeast RSC chromatin remodeler reveals a role for RSC3 and SNF5 homolog 1 in ploidy maintenance. PLoS Genet 3(6): e92. doi:10.1371/journal.pgen.0030092

Introduction

Maintenance of ploidy is crucial for sexual reproduction in eukaryotes because the ploidy changes that take place during gametogenesis require two identical chromosome complements. Polyploid plant, insect, amphibian, and mammalian species have been documented, and various forms of somatic polyploidy have been described, including mammalian hepatocytes, megakaryocytes, and trophoblasts, insect oocyte nurse cells, and plant endosperm [1–3]. At the cellular level, polyploidy usually represents a highly differentiated state, with increased cell size and elevated metabolic activity. To become polyploid, cells enter a process called endocycling. This usually commences by aborting the mitotic cycle anywhere between G2 (endoreduplication) and cytokinesis (endomitosis), followed by replication [2–4]. Depending on the timing of mitotic exit, cells have multiple chromosome sets contained within a single nucleus or they become multinucleate.

Factors known to drive the switch between mitotic cycling and endocycling include S-phase cyclin-Cdk complexes and their regulators [3,5], as well as the replication origin licensing factors Cdc6, Cdt1, and geminin [6–9]. Such specialized cell-cycle transitions can involve switching between expression of protein isoforms, as reported for cyclin D variants in mammalian trophoblasts [10], or they can be restricted to a variation in oscillation of gene expression, as observed for cyclin E in *Drosophila* nurse nuclei [3]. Finally, mutations in multiple components of the yeast spindle pole body (Msp1p, Msp2p, Mob1p, Cdc31p, Ndc1p, and Kar1p), the fungal centrosome, have been reported to result in numerical chromosome doubling events in yeast [11–15].

In order to remodel chromosomes, eukaryotes have evolved multi-subunit protein complexes that can alter chromatin structure covalently, by modifying nucleosomes [16,17], or mechanically, via ATP-dependent chromatin remodeling (SNF2-type ATPases) [18,19]. Within the latter class, the SWI2/SNF2 enzymes are represented in yeast by the Sth1p and Swi2p/Snf2p ATPases that reside in the related multi-subunit complexes "remodels the structure of chromatin" (RSC) [20] and mating type "switching deficient/sucrose non-fermenting" (SWI/SNF) [21,22], respectively. RSC and SWI/SNF complexes are structurally related, sharing three subunits and harboring five paralogs [23,24]. Despite their extensive structural homology, dysfunction of various essential RSC components cannot be compensated for by overexpression of SWI/SNF paralogs, arguing that protein motifs that mediate complex assembly and function differ [20,25]. Furthermore, genetic evidence indicates that SWI/SNF and RSC differ fundamentally with respect to interaction with chromatin since histone and *SPT6* mutations that suppress *snf2Δ* mutants actually enhance conditional $sth1^{S806L,T881M}$ mutant phenotypes [26].

Editor: Bas van Steensel, Netherlands Cancer Institute, Netherlands

Received December 27, 2006; **Accepted** April 20, 2007; **Published** June 1, 2007

A previous version of this article appeared as an Early Online Release on April 20, 2007 (doi:10.1371/journal.pgen.0030092.eor).

Abbreviations: CFU, colony-forming unit; HU, hydroxurea; MBF, *MluI* cell cycle box-binding factor; ORF, open reading frame; RSC, remodels the structure of chromatin; SWI/SNF, mating type switching deficient/sucrose non-fermenting

* To whom correspondence should be addressed. E-mail: c.logie@ncmls.ru.nl

Author Summary

Some molecules responsible for altering the 3-D organization of chromosomes work as complexes of more than ten different proteins, and many are conserved in fungi, plants, and animals. Two such complexes are called "remodels the structure of chromatin" (RSC) in yeast and "switching deficient/sucrose non-fermenting" (SWI/SNF) in man. SWI/SNF is known to inhibit the advent of multiple types of human cancers. Since cancer is a disease whereby cells unduly divide, we sought to define when in the yeast cell division cycle RSC executes essential functions. Using a generic method to induce inactivation of essential proteins in otherwise healthy yeast cells, we found that the RSC complex is important before chromosome replication as well as before chromosome segregation. Interestingly, combining two of the mutations we had generated caused doubling of the entire chromosome complement of yeast. As it is known that such multiplication of the cellular chromosome complements results in an increased malleability of the genetic patrimony, which itself is known to underlie some of the aggressive traits of human cancers, our discovery suggests new models as to why SWI/SNF is such a potent tumor suppressor, and this may in turn provide valuable new inroads for cancer treatment.

To date, genetic and molecular analyses have implicated RSC in a variety of biological processes including chromosome cohesion and transmission, DNA repair, and transcriptional regulation [27–35]. In addition, RSC interacts with a PKC pathway that impinges on cell polarity through Bim1p, a microtubule-associating protein that ensures spindle pole body asymmetry through Kar9p [36,37].

To address fundamental questions with respect to RSC function, we analyzed generic degron alleles of essential RSC subunits. Here, we report that RSC executes essential functions in G1, G2, and mitosis. Strikingly, integral ploidy shifts occurred when degron alleles of the yeast hSNF5 tumor suppressor ortholog *SFH1* [38,39] and the cell cycle–regulated *RSC3* subunits were combined. Combination of the $sfh1^{td}$ and $rsc3^{td}$ alleles with cyclin deletion alleles revealed a strong genetic interaction between the S-phase cyclin gene, *CLB5*, and *RSC3*, indicating a role for Rsc3p in proper S-phase regulation. Furthermore, impairing rereplication control mediated by Clb5p and the replication origin-licensing factor Cdc6p eliminated the requirement for concomitant deregulation of *SFH1* and of *RSC3* to induce ploidy doubling events. Our data implicate RSC in regulation of the G1/S-phase transition and establish an unanticipated role for RSC-mediated chromatin remodeling in ploidy maintenance.

Results

Generation of Conditional Alleles of All Essential RSC Complex–Specific Subunits

In order to investigate the role of RSC in cellular physiology, we utilized an inducible protein degradation system based on fusion of an N-terminal heat-inducible ubiquitin ligase-target peptide ("degron") [40] to the open reading frames (ORFs) of all essential RSC-specific subunits. This included replacement of the endogenous promoters by the P_{Cup1} promoter, resulting in Cu^{2+} driven transcription of the rsc^{td} alleles. The system also included integration of the $P_{Gal1-10}$ promoter at the *UBR1* locus, which encodes the N-end rule E3 ligase Ubr1p, that recognizes the N-terminal

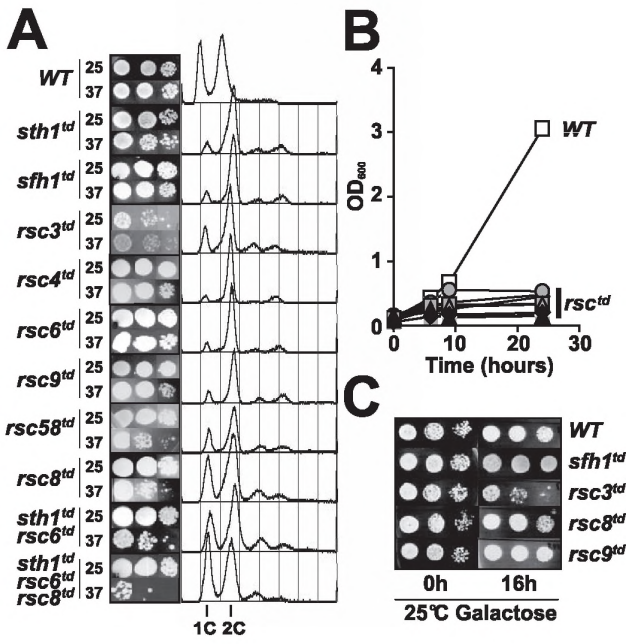

Figure 1. Conditional Depletion of RSC Subunits Terminally Arrests Cells at Multiple Stages of the Cell Cycle

(A) Characterization of yeast strains bearing degron alleles of RSC subunits. Strains were cultured in galactose media at 25 °C (left panel, top lanes) or 37 °C (left panel, bottom lanes) to deplete degron fusions of RSC subunits for 3, 6, and 9 h (only 9 h shown), and a 10-fold serial dilution was spotted onto rich medium and incubated for 3 d at 25 °C (left panel; see Materials and Methods). In parallel, aliquots were taken following depletion and analyzed for DNA content by flow cytometry (right panel). For a more complete set of strains, see Figure S2.

(B) Growth curves under nonpermissive conditions of several strains used in (A) □, Wild type; ■, $sth1^{td}$; ▩, $sfh1^{td}$;◆, $rsc3^{td}$;●, $rsc4^{td}$;■, $rsc6^{td}$;▲, $rsc9^{td}$;▲, $rsc58^{td}$; ◆, $rsc8^{td}$.

(C) Cells were shifted from YEP-glucose medium supplemented with 0.1 mM $CuSO_4$ at 25 °C to YEP-galactose supplemented with 0.1 mM $CuSO_4$ at 25 °C, and 10-fold dilutions were spotted after 0 or 16 h onto glucose containing plates with 0.1 mM $CuSO_4$ and incubated at 25 °C. All strains displayed in this figure contain the P_{gal}::*UBR1* allele.

doi:10.1371/journal.pgen.0030092.g001

arginine residue of the degron fusions [41]. This permits suppression of degron fusion degradation by growing cells in glucose media, which represses the $P_{Gal1-10}$ promoter, and allows priming of degron-fusion degradation by pre-growing cells in galactose media at 25 °C. Thus, this system permits heat shock–induced, polyubiquitin-mediated degradation of existing cellular protein fusions [41].

Cells expressing degron alleles of the essential RSC subunits ($rsc3^{td}$, $rsc4^{td}$, $rsc6^{td}$, $rsc8^{td}$, $rsc9^{td}$, $rsc58^{td}$, $sfh1^{td}$, and $sth1^{td}$) as sole source of that subunit grew at rates comparable to wild-type strains when cultured in glucose at 25 °C, indicating that the degron fusions were functional (unpublished data). Upon induction of ubiquitin ligase Ubr1p expression at 25 °C by galactose, $rsc3^{td}$ strains (but none of the other RSC degron strains) arrested growth, and colony formation was strongly diminished (Figure 1A and 1C). This indicates that Rsc3p is exquisitely sensitive amongst RSC subunits to the presence of the N-terminal degron.

Following incubation of rsc^{td} strains in galactose at 37 °C, growth arrest ensued for all subunits within 3–4 h (Figure 1B). Western blot analysis indicated that degron fusions were depleted to nondetectable levels within 2 h (Figure S1 and

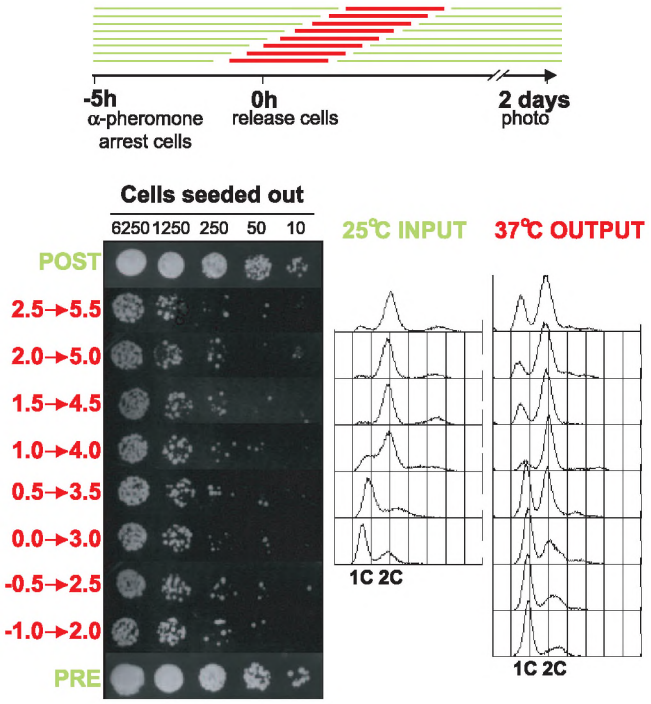

Figure 2. RSC Is Essential during G1

The *MatA, P_{gal}::UBR1, sth1^{td}, rsc6^{td}, rsc8^{td}* strain (YN286) was synchronized in G1 by incubation in α-pheromone (10 μg/ml final) as indicated in the time line (top panel). Incubations at permissive and nonpermissive temperatures are represented by green and red lines, respectively. The α-pheromone was washed out after 5 h and aliquots of cells were shifted from the master culture to 37 °C for 3-h periods as indicated (top panel). CFUs were visualized by seeding 5-fold serial dilutions onto YEP-glucose + $CuSO_4$ plates followed by incubation at 25 °C for 3 d. DNA content was determined by FACS analysis. FACS samples were also taken after 5 h at 37 °C and gave identical profiles as the 3-h samples, indicating that terminal cell-cycle arrests had been reached after 3 h at 37 °C (unpublished data). The "pre" and "post" samples show viability in the 25 °C master culture before and after the experiment, respectively.

doi:10.1371/journal.pgen.0030092.g002

unpublished data) and Sth1p^{TAP} level also decreased (Figure S1), indicating impaired complex integrity. Flow cytometry analysis of cellular DNA content revealed G2/M cell-cycle arrests in *rsc4^{td}, rsc6^{td}, rsc9^{td}*, and *sfh1^{td}* strains (Figures 1A and S2). *sth1^{td}* strains gave variable results, usually yielding almost exclusively G2/M cells, though occasionally significant levels of G1-blocked cells were observed. In contrast, both G1- and G2/M-arrested cells were invariably observed in *rsc8^{td}, rsc58^{td}*, and *rsc3^{td}* strains. Importantly, every combination of RSC degrons that was tested induced both G1 and G2/M arrests (Figures 1A and S2).

Irreversible lethal effects, observed as a decrease in colony-forming units (CFUs) upon seeding-out onto 2% glucose plates and incubation at 25 °C, were more pronounced and occurred earlier in the 37 °C time course in *rsc8^{td}* and *rsc58^{td}* strains, as well as in strains harboring multiple RSC degron fusions (Figure 1A). In the extreme case of the *rsc6^{td}, rsc8^{td}, sth1^{td}* triple degron strain, less than 1% CFUs remained after 3 h of heat shock (Figure 1A), while equivalent fractions of pre- (Figure 1C) and post-replicative (Figure 2C) cells were observed.

Altogether, these data suggest that the cell-cycle phase of arrest correlates with the kinetics of RSC complex inactivation, with G2/M cells being more sensitive to RSC inactivation than G1 cells since G2/M cells accumulate when RSC function is least impaired, as assayed by cell survival.

RSC Is Essential in the G1 Phase of the Cell Cycle

As no essential role has previously been described for RSC during G1, we wished to determine whether the G1 arrest we observed upon RSC depletion (Figures 1A and S2) resulted from functional failure in the course of the preceding cell cycle or whether this reflected a genuine essential function for RSC during G1. To this end, the triple *rsc6^{td}, rsc8^{td}, sth1^{td}* degron combination, which conveyed >99% lethality within 3 h of heat shock (Figure 1A), was employed to deplete RSC from synchronously cycling cells (Figure 2). Cells were grown overnight in galactose at 25 °C and were then blocked in G1 by exposure to α-pheromone (−5 h; boost at −2.5 h). Release into the cell cycle was achieved by removal of pheromone (0 h). Aliquots of synchronized cells were taken at 30-min intervals and incubated for 3-h periods at 37 °C so as to deplete RSC from cells traversing consecutive stages of the cell cycle synchronously. After 3 h at 37 °C, cellular DNA content was determined and cells were seeded-out onto permissive plates to determine viability levels by colony formation (Figure 2). RSC inactivation in synchronized cells proved lethal for >95% of the cells in every case (Figure 2), and RSC inactivation resulted in homogeneous G1 and G2/M arrests, depending on the time when heat shock was applied (Figure 2).

We conclude that RSC executes essential functions in G1 in addition to its essential roles in G2/M. As we did not observe cells arrested in the process of DNA replication (corresponding to the 0.5 h to 3.5 h time point), our experiments suggest that RSC activity is not required per se for chromosome replication. However, we cannot exclude the possibility that a small portion of the genome failed to be replicated upon RSC depletion (Figure 2, 0.5 h to 3.5 h time point).

sfh1^{td} and *rsc3^{td}* Together Induce Single Rounds of Ploidy Doublings

The above analyses indicated that RSC performs crucial functions during mitosis, G1, and G2, and they implicate RSC in proper cell-cycle progression. This perception was further strengthened in the process of generating yeast strains harboring combinations of degron alleles of essential RSC subunits. Whereas most diploid strains heterozygous for two or three degron alleles produced >80% viable spores, diploid strains heterozygous for *sfh1^{td}* and *rsc3^{td}* and homozygous for *P_{gal}::UBR1* yielded less than 10% viable spores (Table S1). This dominant meiotic-lethal phenotype was not due to aberrant ploidy of the parental strains, as both haploid *rsc3^{td}* and *sfh1^{td}* strains displayed the expected haploid DNA contents (Figure 1A). Furthermore, the *sfh1^{td}* and *rsc3^{td}* strains were able to individually mate with other haploid *rsc^{td}* strains to produce diploids that produced >80% viable spores with the expected segregation frequencies of heterozygous markers (Table S1).

We tested the involvement of the *P_{gal}::UBR1* allele by mating a *UBR1, sfh1^{td}* strain to a *UBR1, rsc3^{td}* strain. These diploids were fertile (64% viable progeny); however, none of the surviving progeny harbored both the *rsc3^{td}* and the *sfh1^{td}* degron alleles (Table 1). This demonstrates that the dominant meiotic-lethal phenotype displayed by double heterozygous *rsc3^{td}/RSC3, sfh1^{td}/SFH1, P_{gal}::UBR1/P_{gal}::UBR1* diploids was due to repression of *UBR1* expression. This suggests that RSC and

Table 1: Synthetic Lethality between *rsc3*^{td} and *sfh1*^{td}

Frequency	*SFH1, RSC3*	*sfh1*^{td}*, RSC3*	*SFH1, rsc3*^{td}	*sfh1*^{td}*, rsc3*^{td}
Observed	37	30	31	0
Expected if not SL	38	38	38	38
Expected if SL	38	38	38	0

UBR1, sfh1^{td}, and *UBR1, rsc3*^{td} strains of opposing mating type were mated, and resulting diploid strains were induced to sporulate. Spores from 38 asci were analyzed for colony formation and segregation of *sfh1*^{td} and *rsc3*^{td} alleles, as well as several auxotrophic markers. SL, synthetic lethal.

doi:10.1371/journal.pgen.0030092.t001

Ubr1p, or physiological Ubr1p substrates [42], are part of genetic pathways that are redundant to some extent or that form one large pathway in meiosis.

Interestingly, the dominant meiotic-lethal phenotype of diploids homozygous for P_{gal}*::UBR1* and heterozygous for *rsc3*^{td} and *sfh1*^{td} could be rescued by inclusion of a single copy of *rsc9*^{td}, but not by inclusion of *sth1*^{td}, *rsc6*^{td}, *rsc8*^{td}, or *rsc58*^{td} alleles (unpublished data). Remarkably, we observed that every single descendant spore of the triple heterozygous diploids that bore both the *sfh1*^{td} and the *rsc3*^{td} alleles gave rise to large, mono-nucleated cells that had a diploid DNA content, regardless of the presence of the *rsc9*^{td} allele (>50 tetrads analyzed). The DNA profile of one *sfh1*^{td}, *rsc3*^{td} nonparental di-type tetrad is shown in Figure 3A. Both progeny that inherited the *rsc3*^{td} and the *sfh1*^{td} alleles have 2C + 4C DNA contents, while the two other spores display the 1C + 2C DNA content expected for haploid yeast. The endodiploid *sfh1*^{td}, *rsc3*^{td} strains responded to mating pheromone (unpublished data) and could mate to produce tetraploid strains (4C/8C, Figure 3B). The ploidy shift took place after meiotic segregation of the chromosomes because inheritance of all the heterozygous chromosomal loci obeyed the Mendelian 2:2 frequency.

In order to test whether endodiploid strains could be generated independently of passage through meiosis, we performed endogenous locus replacement experiments in haploid cells. When *UBR1, rsc3*^{td} strains were transformed with vectors to convert the wild-type *SFH1* allele to *sfh1*^{td}, 10% of the resulting colonies were haploid, 80% were diploid, and 10% also harbored tetraploid cells ($n = 48$, Figure 3C and Table 2). Thus, the endocycle induced by the *rsc3*^{td} and *sfh1*^{td} alleles could also occur independently of meiosis. Transformation of *UBR1, sfh1*^{td} haploid strains with the *rsc3*^{td} locus conversion construct yielded fewer endodiploid clones (4%; $n = 48$, Table 2). This suggests that the presence of *rsc3*^{td} primed cells to undergo a ploidy shift, a fact that may well relate to the sensitivity of *rsc3*^{td} strains (but no other *rsc*^{td}-containing strains) to overexpression of the E3 ligase Ubr1p at 25 °C (Figure 1C).

To assess the role of *UBR1* in *rsc3*^{td} + *sfh1*^{td} mediated ploidy shifts, the above endogenous locus replacement experiment was also performed in P_{gal}*::UBR1* cells grown in glucose. Inhibition of *UBR1* significantly reduced the frequency of observed ploidy shifts (Table 2), consistent with an ancillary role for Ubr1p in this phenomenon.

We conclude that together, degron alleles of *RSC3* and *SFH1* disrupt a facultative cell-cycle process that is crucial to maintain ploidy levels in yeast. Furthermore, the fact that ploidy shifts only took place once or twice strongly suggests that a third biological parameter is involved, and that this parameter was triggered in both the endogenous locus conversion and the meiotic segregation experiments.

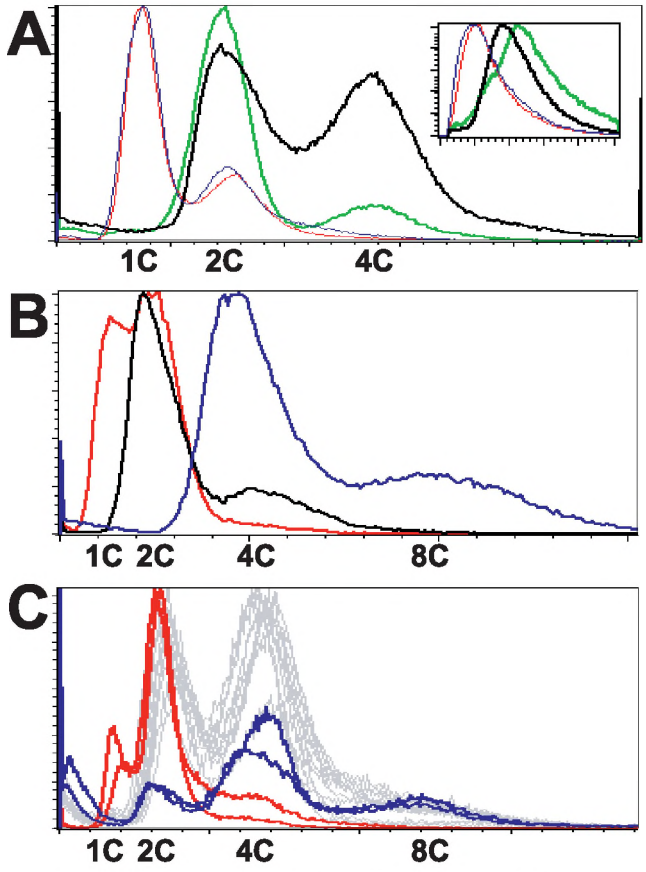

Figure 3. Post-Meiotic and Mitotic Ploidy Doubling of *sfh1*^{td}, *rsc3*^{td} Cells

(A) FACS analysis of the DNA content of the four spores of a single representative tetrad derived from a *SFH1/sfh1*^{td}*, RSC3/rsc3*^{td}*, RSC9/rsc9*^{td}*,* P_{gal}*::UBR1/*P_{gal}*::UBR1* diploid. The genotypes of the spores are *SFH1, RSC3, RSC9,* P_{gal}*::UBR1* (blue), *SFH1, RSC3, rsc9*^{td}*,* P_{gal}*::UBR1* (red), *sfh1*^{td}*, rsc3*^{td}*, RSC9,* P_{gal}*::UBR1* (green), *sfh1*^{td}*, rsc3*^{td}*, rsc9*^{td}*,* P_{gal}*::UBR1* (black). Inset: Light scatter plots indicating cell sizes.

(B) Tetraploid strain (blue) derived from mating of two endodiploids (black). For comparison, a haploid was included (red).

(C) FACS analysis of clones generated by transformation of a *rsc3*^{td} strain with a *sfh1*^{td} allele. Haploid clones are indicated in red, endodiploids in gray, and tetraploids in blue.

doi:10.1371/journal.pgen.0030092.g003

RSC Genetically Interacts with the Cyclin-Dependent Kinase Cdc28p/Cdk1p

In budding yeast, cell-cycle progression is orchestrated by a single cyclin-dependent kinase, Cdc28p/Cdk1p [43]. As we found RSC to be crucial for passage through multiple stages of the cell cycle, we wished to assess functional interactions between RSC and Cdc28p/Cdk1p. To this end, we employed a *cdc28*^{td} degron allele [40]. Upon Ubr1p overexpression, the *cdc28*^{td} allele led to a severe decrease in CFUs. This phenotype was exacerbated by inclusion of the *sth1*^{td} allele (Figure 4), arguing that hypomorphic alleles of RSC and Cdc28p/Cdk1p genetically interact. This notion was further substantiated by the observation that *sth1*^{td} cells overexpressing *Saccharomyces cerevisiae WEE1 (SWE1),* a tyrosine kinase that controls mitosis entry by inhibition of Cdc28p/Cdk1p activity [43,44], were

Table 2: Ploidy Alterations by Endogenous Locus Conversion

Strain	Integrate	*UBR1*			P_{gal}::*UBR1*		
		1C	2C	4C	1C	2C	4C
WT	$sfh1^{td}$	100	0	0	100	0	0
$rsc3^{td}$	$sfh1^{td}$	10	80	10	48	52	0
WT	$rsc3^{td}$	100	0	0	100	0	0
$sfh1^{td}$	$rsc3^{td}$	96	4	0	100	0	0

Wild-type (WT), $sfh1^{td}$, or $rsc3^{td}$ strains were transformed with endogenous locus conversion constructs for $sfh1^{td}$ or $rsc3^{td}$ and selected for integration of the respective alleles. Resulting transformants were analyzed for DNA content by flow cytometry (see Figure 3) and results are shown as percentage of colonies analyzed ($n = 48$). Experiments were performed using cells expressing endogenous levels of *UBR1 (UBR1)*, or cells repressing *UBR1* expression (P_{gal}::*UBR1*) as indicated.

doi:10.1371/journal.pgen.0030092.t002

also exquisitely sensitive to overexpression of Ubr1p at 25 °C (Figure 4). Together, these synthetic lethal effects demonstrate that the RSC catalytic ATPase subunit Sth1p genetically interacts with the cyclin-dependent kinase pathway.

Specific Genetic Interaction between the $rsc3^{td}$ Allele and the *CLB5* S-Phase Cyclin

Our results suggest that a specific cell-cycle process is impaired in cells that harbor both the $sfh1^{td}$ and $rsc3^{td}$ degron alleles, and that this could relate to a specific cyclin-dependent kinase pathway. In order to map this process, we mated P_{gal}::*UBR1*, $rsc3^{td}$ and P_{gal}::*UBR1*, $sfh1^{td}$ strains to a panel of deletion strains that lacked any one of the nine Cdk1p/Cdc28p associated cyclins and assessed spore viability on glucose plates. This analysis did not reveal significant genetic interactions between $sfh1^{td}$ and any of the cyclin deletions (Figure 5A). In the case of the $rsc3^{td}$ allele, however, a significant loss of spore viability was observed upon combination with the *clb5*Δ allele. As a matter of fact, we did not recover a single *UBR1* clone that harbored both the *clb5*Δ and the $rsc3^{td}$ alleles, indicating that the latter alleles form a lethal combination, and that lethality was suppressed by repression of Ubr1p levels (using the P_{gal}::*UBR1* allele; Figure 5B). Other *UBR1*, cyclin deletion, $rsc3^{td}$ double mutants were recovered with the expected frequency, demonstrating a specific interaction between *clb5*Δ and $rsc3^{td}$. We conclude that the $rsc3^{td}$ allele impairs a cell-cycle process that also relies on Clb5p. As this cyclin is known to control late S-phase progression [43,45,46], this suggests that an important S-phase event is disrupted by the $rsc3^{td}$ allele.

The Rereplication Control Machinery Antagonizes $rsc3^{td}$-Mediated Ploidy Shifts

Endocycling of eukaryotic cells (e.g., mammalian hepatocytes and megakaryocytes) commonly relies on alternative regulation of genes essential for replication control, such as G1/S cyclins, Cdc6, geminin, and Cdt1 [3,6,7,9]. We therefore assessed the role of the yeast origin licensing factor Cdc6p [47,48] in ploidy shifts induced by $rsc3^{td}$ and $sfh1^{td}$. As Cdc6p is an essential protein, we attenuated its cellular levels using a strain expressing *CDC6* solely from a methionine repressible promoter [49]. Cells were incubated in the presence of 2 mM methionine for 45 min to repress *CDC6* transcription, and then they were made competent for transformation. These cells were transformed with control constructs, or with endogenous locus conversion constructs for the $sfh1^{td}$ or $rsc3^{td}$ alleles. Clones were then selected at 25 °C on glucose

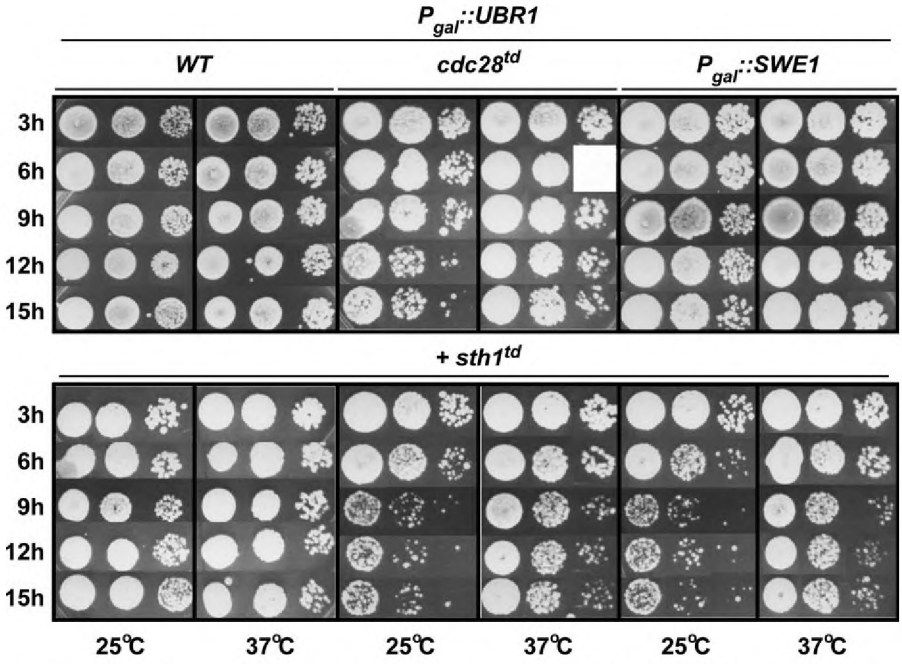

Figure 4. Synthetic Sickness Phenotype of $sth1^{td}$, $cdc28^{td}$, and $sth1^{td}$, P_{gal}::*SWE1* Double Mutants

Haploid yeast strains harboring P_{gal}::*UBR1* and combinations of $sth1^{td}$ and $cdc28^{td}$ ($cdk1^{td}$) or P_{gal}::*SWE1* were analyzed for their ability to form colonies after growth in galactose for the indicated times at the indicated temperatures, by seeding-out 10-fold serial dilutions of an equal number of cells onto solid glucose medium containing 0.1 mM $CuSO_4$. Note the dramatically increased severity of the lethal phenotypes of $cdc28^{td}$ and P_{gal}::*SWE1* alleles when they were combined with $sth1^{td}$. The data shown are from one experiment and are representative of at least three independent experiments.

doi:10.1371/journal.pgen.0030092.g004

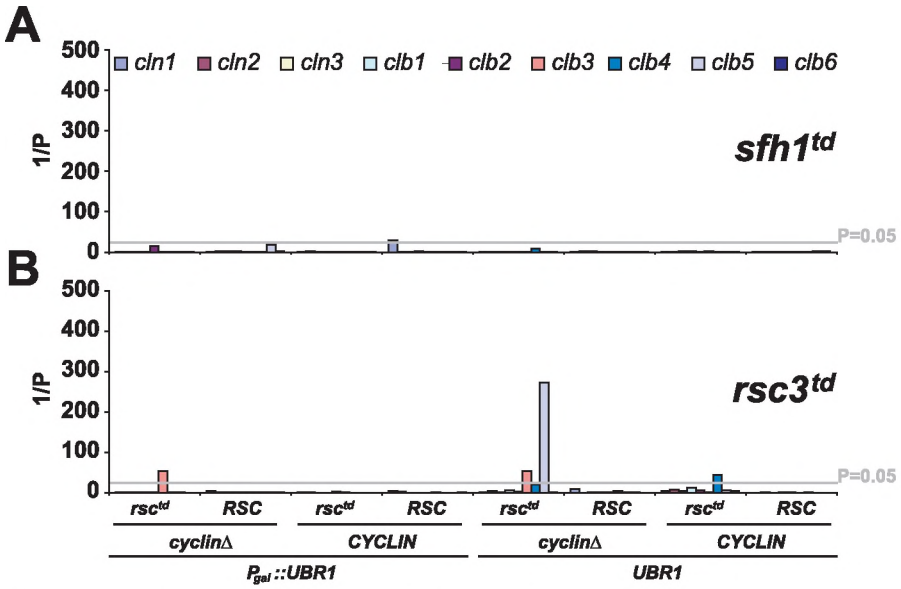

Figure 5. Synthetic Lethality of *UBR1*, *clb5*Δ, *rsc3*^{td} Spores

Haploid yeast strains harboring P_{gal}::*UBR1* and either *sfh1*^{td} (A) or *rsc3*^{td} (B) were crossed to strains harboring deletion of any one of the nine *S. cerevisiae* cyclin genes: *CLN1*, *CLN2*, *CLN3*, *CLB1*, *CLB2*, *CLB3*, *CLB4*, *CLB5*, or *CLB6*. For each cross, three independently obtained diploids were induced to sporulate and between 16 and 53 tetrads were microdissected. Spore survival ranged from 76% to 96% and from 53% to 89% for the *sfh1*^{td} and *rsc3*^{td} harboring diploids, respectively. Chi square values for the cosegregation frequencies of the cyclin deletion, the P_{gal}::*UBR1*, and the *sfh1*^{td} or *rsc3*^{td} alleles were calculated for each cross. The probability of obtaining the number of observed spores is plotted for each indicated genotype. None of the segregating loci under scrutiny are located on the same chromosome. The observed deviation from the expected number of *UBR1*, *clb5*Δ, *rsc3*^{td} progeny reflected a fully penetrant inability of such spores to form a colony.

doi:10.1371/journal.pgen.0030092.g005

plates lacking methionine so as to restore *CDC6* transcription. Control cells that had not been depleted of Cdc6p yielded exclusively haploid clones upon conversion of the *RSC3* or *SFH1* loci to the corresponding degron alleles (Figure 6). In contrast, ploidy shifts were efficiently induced in cells depleted of Cdc6p upon conversion of the *RSC3* locus to *rsc3*^{td}, but not upon conversion of the *SFH1* locus to *sfh1*^{td} ($n = 60$; 60% and 0%, respectively, Figure 6). Thus, temporary depletion of Cdc6p appears to phenocopy the *sfh1*^{td} allele but not the *rsc3*^{td} allele.

Next, we turned to the cyclin Clb5p. Besides a role in spindle pole body maturation and duplication [50,51], Clb5p plays a dual role in replication regulation as it is required for proper timing of S-phase initiation, as well as to prevent re-initiation of replication forks that have already fired [52]. Furthermore, deregulation of *CLB5* levels has been associated with the occurrence of endoreduplication [52]. Wild type and *clb5*Δ strains were transformed with the same constructs as above. In this experimental setup, and contrary to meiotic segregation, *UBR1*, *rsc3*^{td}, *clb5*Δ mutants could be recovered. Analysis of the resultant *rsc3*^{td} clones ($n = 72$) showed efficient ploidy doubling in the *clb5*Δ background (74%; Figure 6) in contrast to control constructs. Conversion of *SFH1* to *sfh1*^{td} in the *clb5*Δ background could also produce endodiploid clones, though at a much lower frequency (1%, Figure 6). Taken together, this indicates that the cellular rereplication inhibition pathway that depends on *CLB5* and *CDC6* [48,52] antagonizes the effects of the degron alleles of *RSC3* and *SFH1*.

RSC and Transcriptional Activity of the *CLB5* Locus

Previous observations indicate that RSC is recruited to the *CLB5* promoter [27], and *CLB5* induction was observed in microarray experiments using a *rsc3* allele [53]. To further assess the role for RSC in regulation of *CLB5* expression, we impaired S-phase progression by exposure to hydroxyurea (HU), an inhibitor of deoxyribonucleotide synthesis. HU treatment activates the S-phase checkpoint that signals through Rad53p and phosphorylation of various targets, including Swi6p, thus culminating in inhibition of S-phase progression [54–56]. Following exposure to HU for 3 h we monitored association of RSC with a number of loci by Sth1p^{TAP} chromatin immunoprecipitation (Figure 7A), and we assessed expression of *CLB5* and *TPS3* (Figure 7B). HU treatment resulted in up to 3-fold increased association of Sth1p with the *CLB5* promoter (Figure 7A), concomitant with repression of *CLB5* expression (Figure 7B), much as reported for *HTA1* (Figure 7A, [27]). The increased association of RSC complexes with the *CLB5* and *HTA1* promoters upon HU treatment was specific, as no such effects were observed at *TPS3*, *FUR4*, *CEN4*, at an ORF-free chromosomal element on Chromosome I *(ORF-FREE)* or in the *CLB5* ORF (*CLB5-ORF*, Figure 7A and 7B). Taken together, these results correlate increased binding of RSC to the *CLB5* promoter with inactivation of this locus upon HU treatment (Figure 7A and 7B) and further implicate RSC in transcriptional control of *CLB5* expression.

Discussion

The RSC ATP-dependent nucleosome remodeling complex [20] encompasses 17 subunits, and the mutually exclusive paralogs Rsc1p and Rsc2p define two RSC isoforms [57]. The Rsc3p/Rsc30p heterodimer [20,53] preferentially associates with the Rsc1p-bearing RSC isoform (Campsteijn et al., unpublished data). Here, we analyzed RSC requirement

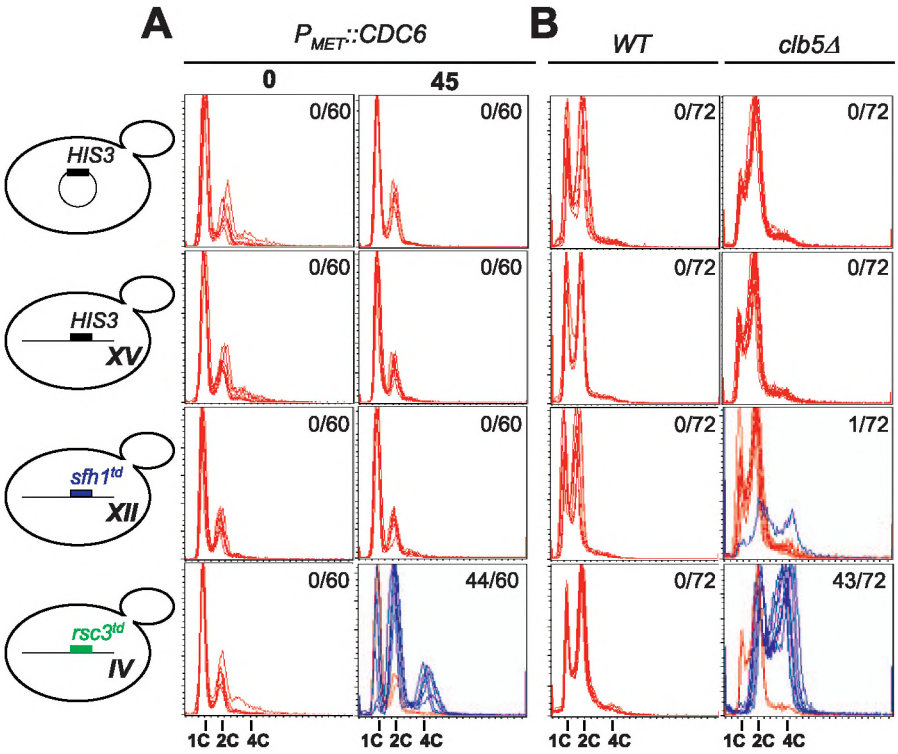

Figure 6. Implication of Replication Control in RSC-Induced Ploidy Shifts

(A) P_{met}::*CDC6, cdc6Δ* cells (and wild-type cells, unpublished data) were cultured in the absence (0 min) or presence (45 min) of 2 mM methionine to repress *CDC6* expression, and cells were made competent for transformation. After transformation with the indicated constructs (left panel), cells were seeded on plates lacking methionine to induce *CDC6* expression. DNA content of resulting transformants is shown ($n = 60$, cumulative of three independent experiments). Haploid clones are depicted in red, endodiploids in blue, and number of endodiploids is shown as an inset.

(B) Wild-type and *clb5Δ* cells were transformed with the constructs as indicated (left panel). DNA content of resulting colonies is shown ($n = 72$). The color scheme is the same as in (A). These data represent the cumulative results of three independent experiments.

doi:10.1371/journal.pgen.0030092.g006

during the course of the cell cycle using conditional degradation alleles (N-degrons) of all essential RSC-specific subunits. We find that RSC controls cell-cycle progression at multiple stages of the cell cycle and uncovered a strong genetic interaction between RSC and cyclin-dependent kinase 1 (Figure 4).

RSC Functions in G2/M

We temporally dissected the mitotic requirement for RSC by depleting RSC subunits from cells harboring G2 or mitosis checkpoint mutations (Figure S3). In keeping with a role for RSC in G2 and mitotic prophase, RSC degron alleles synergized with overexpression of the G2/M transition regulator *SWE1* [43,44], and the same RSC alleles were partially epistatic to a degron allele of the spindle checkpoint factor *CDC20* [58] (Figure S3). On the other hand, a degron allele of the mitotic exit network kinase *CDC15* [59] weakly suppressed the lethal effects of those same RSC subunit degron alleles (Figure S3). Collectively, these results indicate that RSC activity is central to achieving a proper mitosis and that RSC appears to be somewhat more important before the metaphase/anaphase transition than afterward (Figure S3). While these results are consistent with published reports, it remains to be seen whether the essential role of RSC in G2 and in mitosis relates to a role for RSC in gene expression [27,28,35,53], in higher order chromatid structure [32–34,60,61], or both.

RSC Functions in G1

Several lines of evidence provided here argue that RSC functionally intersects with regulation of the G1/S-phase transition. First, cells deprived of RSC arrest in G1 (Figures 1 and 2). Second, we and others [27] find that RSC associates with several *MluI* cell cycle box-binding factor (MBF) targets including the *HTA1/HTB1* and *CLB5* promoters (Figure 7, unpublished data). Both *HTA1/HTB1* and *CLB5* are expressed during the G1/S transition and association of RSC correlates with transcriptional inactivity of these loci (Figure 7, [27]). Third, we discovered that the $rsc3^{td}$ allele is synthetic lethal with a deletion allele of the cyclin *CLB5* when combined via meiotic segregation (Figure 5). When these two alleles were combined by endogenous locus conversion through DNA transformation, surviving clones could be recovered, however, and the resulting *clb5Δ*, $rsc3^{td}$ strains underwent integral ploidy increases (Figure 6). This was also the case when the replication origin licensing factor Cdc6p was transiently depleted (Figure 6). As these genes are crucial for G1/S-phase transition, this very strongly suggests that RSC plays an important role in ploidy maintenance when this stage of the cell cycle is perturbed.

Consistent with this notion, RSC has been reported to interact physically with Swi6p [62], a component of the central heterodimeric G1/S transcription regulators MBF (with Mbp1p) and SBF (with Swi4p), which are considered to be the functional analogs of mammalian E2Fs [63]. Finally,

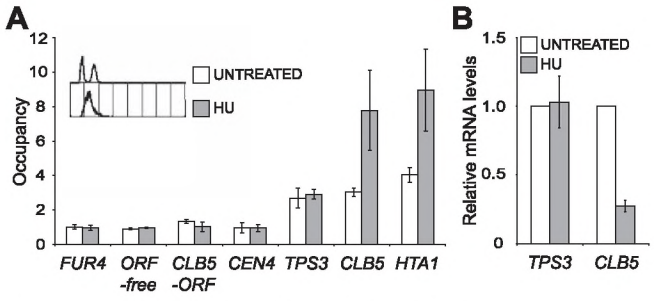

Figure 7. Transcriptional Regulation of *CLB5* by RSC

(A) RSC association with the *CLB5* and *HTA1/HTB1* promoters is increased upon HU treatment. Strains were exposed for 3 h to HU (150 mM) at 30 °C. Cross-linked chromatin was immunoprecipitated using IgG beads (see Materials and Methods), and recovery of indicated fragments was assessed by quantitative PCR. Recovery is shown as fold over the average of RSC occupancy at the *FUR4* promoter (which does not bind RSC, [27]) and at an ORF-free region on Chromosome I (positioned between *YAR053W* and *YAR060C*, [27]). Typically, recovery ranged between 0.1%–0.3% of input for the *CLB5* promoter. The DNA profiles of cells upon harvesting are shown as an inset. Values are the average of three independent experiments using an $STH1^{TAP}$ allele and standard deviations are indicated.

(B) RSC functions as a repressor of *CLB5* expression. Expression levels of the RSC targets *CLB5* and *TPS3* were assessed using quantitative PCR in HU-treated cells and untreated cells. Data are normalized to total RNA concentrations, as well as to the expression levels of these genes in untreated cells and represent the average of three independent experiments.

doi:10.1371/journal.pgen.0030092.g007

rsc1 cells were shown to display a large cell phenotype that is indicative of impaired cell-cycle entry as has been observed in *cln3, bck2, swi4,* and *swi6* strains [64].

RSC Has a Facultative Role in Ploidy Maintenance

The endocycle phenotype we observe in $sfh1^{td}$, $rsc3^{td}$ double mutants underscores the important role of RSC in proper cell-cycle progression. The endocycles occur under conditions when the degron fusions were least affected since the levels of the degron-activating ubiquitin ligase Ubr1p were repressed by glucose and since the yeast were kept at 25 °C to keep the $DHFR^{ts}$ degron fragment folded (Figure 3A) [40,41]. The ploidy shifts must therefore arise from rather subtle functional deregulation of RSC. It is known that a fraction of Sfh1p is phosphorylated during G1 and this is thought to induce Sfh1p dissociation from RSC [65]. In keeping with this observation, we find that $Sfh1p^{td}$ does not stably associate with RSC and that it is readily depleted from the complex upon Ubr1p overexpression (Figure S4). Furthermore, we found that Rsc3p is actively degraded in late S-phase (Campsteijn et al., unpublished data). The fusion of an N-degron to Rsc3p could thus artificially induce $Rsc3p^{td}$ degradation in an untimely fashion, in line with the exquisite sensitivity of $rsc3^{td}$ cells to increased levels of Ubr1p, even at 25 °C (Figure 1A and 1C). We therefore propose that timely regulation of Sfh1p during G1-phase and of Rsc3p during S-phase are imperative to maintain ploidy constant in germinating spores, as well as in cells that have undergone the lithium-mediated DNA transformation procedure. Although it remains unclear at what stage $sfh1^{td}$, $rsc3^{td}$ cells abort the mitotic cycle and re-enter S-phase, the mono-nucleate nature of our endodiploid strains indicates that the endodiploidization event precedes completion of nuclear division.

We found that conversion of *RSC3* to $rsc3^{td}$ in a strain (S288c) deleted for Mbp1p resulted in very slow growing $mbp1\Delta$, $rsc3^{td}$ double mutant clones that underwent cycles of endoreduplication at a steady rate, yielding a heterogeneous population of cells with increasing ploidy state (Figure S5). Together with the functional link between RSC and *CLB5*, our data therefore indicate that RSC interacts with the MBF/SBF controlled transcriptional G1/S cell-cycle progression program. As MBF is thought to function by restricting expression of numerous genes involved in control of DNA replication to G1 (including *CLB5*) [66], it is possible that simultaneous interference with transcriptional regulation by RSC and MBF compromises necessary oscillations in expression pattern of multiple MBF target genes, resulting in reduced cell-cycle phase identity, and, under specific environmental conditions, in ploidy shifts.

Our experiments suggest that both *CLB5* deletion (Figure 6) and *CLB5* derepression (Figure 7) could aid in the induction of ploidy shifts. These opposing observations can be reconciled by the requirement for simultaneous deregulation of multiple MBF-target genes to observe ploidy doublings, as well as by the fact that Clb5p is required for both activation and inactivation of pre-replication complexes [48,52,67–69]. As such, diminished or untimely oscillation in expression level rather than over- or underexpression would result in ploidy shifts, a phenomenon that has been reported for the S-phase cyclin E in *Drosophila* nurse nuclei [3]. This hypothesis is consistent with the observation that hyperstabilization of *CLB5* mRNA suffices to induce ploidy shifts [52].

Finally, we note that *CDC6* expression, which normally peaks during late mitosis, has been reported to peak in a MBF-dependent fashion at the G1/S transition only in cells that have not undergone a recent mitosis [49,70]. As this would be the case following spore germination or cell transformation by the lithium procedure, this may therefore account for the single round of ploidy shifts observed here and for the observed lack of RSC-association with the *CDC6* promoter in cycling cells (unpublished data).

Role of the P_{gal}::*UBR1* Allele in Ploidy Shifts

It is known that Ubr1p participates in cohesin degradation in mitosis [42]. However, our results indicate that the effects of the P_{gal}::*UBR1* allele in our experiments were largely mediated through Ubr1p's role in polyubiquitylation of the N-terminal degron fusions we studied. For instance, repressing Ubr1p levels suppressed rather than enhanced the occurrence of ploidy shifts in $rsc3^{td}$, $sfh1^{td}$ strains (Table 2). Furthermore, repressing Ubr1p expression through P_{gal}::*UBR1* suppressed rather than enhanced the synthetic lethal interaction between $rsc3^{td}$ and $clb5\Delta$ (Figure 5B). However, since the dominant meiotic-lethal phenotype displayed by double heterozygous $rsc3^{td}$/*RSC3*, $sfh1^{td}$/*SFH1*, P_{gal}::*UBR1*/P_{gal}::*UBR1* diploids was due to repression of UBR1 expression (Table 1), our results do suggest that RSC and Ubr1p are part of genetic pathways that are redundant to some extent or that form one large pathway in meiosis.

Conclusion

Our experiments indicate that the $rsc3^{td}$ and $sfh1^{td}$ degron alleles interfere in synergistic ways with cell-cycle progression resulting in environmentally conditioned ploidy shifts. These results formally implicate RSC in ploidy maintenance. The RSC complex has previously been implicated in multiple

molecular processes, including regulation of chromatid cohesion [32], DNA damage response [29–31], nucleocytoplasmic transport [28,71], and transcription control [27,28,35,53,72]. Furthermore, and underscoring the complexity of RSC function, viable RSC subunit deletion strains have been identified that display long *(npl6Δ, htl1Δ,* and *ldb7Δ)* or short *(rsc2Δ)* telomeres, hinting toward ambivalent roles for RSC in maintenance of telomere length [73,74], a process that occurs in late S-phase [75]. In light of the pleiotropic physiological functions of RSC, further dissecting RSC-mediated ploidy control will require a detailed understanding of the roles and modes of regulation of individual RSC subunits, as well as understanding the functional interplay of the various processes that rely on RSC.

The functions we ascribe here to RSC, namely ploidy maintenance and control of G1/S-phase transition, appear conserved for human RSC-like complexes [76–81]. Interestingly, it has been shown that mutant forms of the human ortholog of *SFH1,* the tumor suppressor *INI1/hSNF5* [38,39,82,83], can induce the appearance of tetraploid cells [76,81]. Thus, an ancient RSC-dependent ploidy doubling inhibition mechanism may have been recruited in the course of animal evolution to avert incipient cancer.

Materials and Methods

Yeast strains, plasmids, and culturing. With the exception of the S288c *mbp1Δ* strain (Figure S5) and the S288c cyclin deletion strains (Figure 5), all the yeast used here were descendants of W303 strains. Degrons were introduced in diploid yeast (YN106) by ends-in homologous recombination of plasmids at the endogenous loci (Table S2). Plasmid details are available on request. Verification of the integration events was based on PCR analysis and western blot detection of the modified gene products. For sporulation, diploids were grown overnight on YEP-10% glucose agar plates and sporulated on 1% KAc, 40 μg/ml adenine agar plates. Degron strain were grown overnight in 5 ml of the appropriate SD-glucose amino acid dropout medium, supplemented with 40 μg/ml adenine, 0.1 mM $CuSO_4$ at 25 °C. The cells were then seeded into a second overnight culture in YEP supplemented with 2% galactose. For depletion, cells were diluted to 2.10^5 cells/ml into YEP 2% galactose, with or without 0.1 mM $CuSO_4$, and incubated at 25 °C or 37 °C. At the indicated times, 5 μl of cells and 5- or 10-fold serial dilutions were spotted onto YEP plates supplemented with 2% glucose, 40 μg/ml adenine, and 0.1 mM $CuSO_4$. The plates were incubated at 25 °C and pictures were taken after 2–4 d. For DNA damage experiments (Figure 7), cells were cultured in nonselective media at 30 °C to an optical density of 0.6, followed by exposure to 150 mM HU (Sigma-Aldrich, http://www.sigmaaldrich.com) for 3 h.

Flow cytometry analysis. Cells were grown in nonselective medium overnight, pelleted, and collected into 70% ethanol and kept at least 2 h at 20 °C. Subsequently, cells were suspended into 50 mM sodium citrate, sonicated briefly, treated for 2 h with 0.2 mg/ml RNase A at 37 °C, and DNA was stained with 1 μM Sytox dye (Molecular Probes, http://www.probes.invitrogen.com). DNA content was quantified at FL1 on a Becton-Dickinson (http://www.bd.com) Calibur fluorescence activated cell sorter.

Chromatin immunoprecipitation, RNA extraction, and quantitative PCR. Chromatin was prepared as described [84] with several modifications. Cells (20–40 ml) were treated with 1% formaldehyde for 15–20 min at room temperature under constant rotation. Glycine was added to a final concentration of 330 mM and incubation continued for an additional 5–10 min. Cells were gently washed three times with cold TBS. The remaining cell pellet was resuspended in lysis buffer (FA-lysis buffer complemented with 1% Triton X-100 and 1 mM DTT) and lysis was performed using glass beads (2-h vortexing on a vortexgenie 2, Scientific Industries, http://www.scientificindustries.com). The obtained lysate was sonicated on ice (four times, 20-s pulses, with 40-s intervals) and clarified by centrifugation. For immunoprecipitation, typically, 400-μl chromatin solution was incubated overnight with 15 μl IgG Sepharose 6 Fast Flow bead suspension (Stratagene, http://www.stratagene.com) prewashed in lysis buffer + 0.1% BSA. Precipitates were washed (5 min) twice with lysis buffer, twice with lysis buffer at 500 mM NaCl, once with 10 mM Tris (pH 8.0), 0.25 M LiCl, 1 mM EDTA, 0.5% DOC, and 0.5% NP40, and once with TE (10 mM Tris [pH 8.0], 1 mM EDTA). Immunoprecipitated material was eluted for 10 min at 65 °C in 400 μl 25 mM Tris (pH 7.5), 10 mM EDTA, and 0.5% SDS. Decrosslinking was done for 4–5 h at 65 °C, and DNA was purified by phenol extraction followed by ethanol precipitation in the presence of 20 μg glycogen.

RNA was extracted with hot acid-phenol: chloroform and cDNA synthesis was carried out using 2 μg of total RNA.

Quantitative PCR was performed in a Bio-Rad (http://www.bio-rad.com) MyiQ Single Color Real-Time PCR Detection System using a 2× iQ SYBR Green Supermix. For ChIP, 1/50 of the immunoprecipitated material was used and abundance of immunoprecipitated fragments was compared to 1% input. For cDNA, 1/25 of total cDNA was used and values were normalized as indicated.

Supporting Information

Figure S1. Depletion of $Rsc8p^{td}$ Compromises RSC Integrity

A *rsc8^{td}, STH1^{TAP}* strain (YN438) was grown overnight in YP-Gal medium containing 0.1 mM $CuSO_4$ at 25 °C and was subsequently shifted to YP-Gal medium at 37 °C to induce degradation of $Rsc8p^{td}$. Aliquots were harvested at the indicated time points and equal amounts of whole cell extracts were analyzed by western blot. $Rsc8p^{td}$ was visualized using anti-HA mouse antibody and $Sth1p^{TAP}$ using peroxidase-conjugated anti-peroxidase rabbit antibody (Sigma-Aldrich).

Found at doi:10.1371/journal.pgen.0030092.sg001 (786 KB PDF).

Figure S2. Simultaneous Depletion of Multiple RSC Degrons Invariably Yields G1 and G2/M Arrests

Indicated strains were incubated under nonpermissive conditions for 4 h after which DNA content was determined by FACS analysis. To assess colony-forming potential, strains were incubated for 2, 6, 9, or 12 h under nonpermissive conditions, after which 5-fold serial dilutions of the cultures were spotted on YP-glucose plates containing 0.1 mM $CuSO_4$, followed by incubation at 25 °C and photography (inset).

Found at doi:10.1371/journal.pgen.0030092.sg002 (355 KB PDF).

Figure S3. RSC Requirement after Replication

(A–C) Strains harboring the indicated *rsc^{td}* alleles and/or the conditional cell division cycle alleles for *CDC15, CDC20,* or *SWE1* were cultured as described (Materials and Methods), followed by shift to 37 °C in galactose medium lacking $CuSO_4$. Aliquots of these cultures were seeded under permissive conditions at the indicated time points.

(D–F) Indicated strains were incubated for 9 h under nonpermissive conditions, after which cellular DNA content was assessed by FACS analysis.

Found at doi:10.1371/journal.pgen.0030092.sg003 (3.7 MB PDF).

Figure S4. $Sfh1p^{td}$ Association with RSC Depends on Ubr1p Levels

RSC was purified using an *STH1^{TAP}* allele from wild-type (YN400) or *sfh1^{td}* (YN453) strains following overnight culturing at 25 °C in the presence of $CuSO_4$ in glucose (Glu) or galactose (Gal) media to repress or overexpress Ubr1p, respectively. Equal amounts of RSC were loaded in each lane. The position of $Sfh1p^{td}$ (empty arrowhead) is indicated. All strains used in this figure contain the P_{gal}*::UBR1* allele. Note that loss of $Sfh1^{td}$ did not perceptibly affect complex integrity.

Found at doi:10.1371/journal.pgen.0030092.sg004 (532 KB PDF).

Figure S5. Implication of Mbp1p in RSC-Mediated Ploidy Shifts

S288c *mbp1Δ* cells were transformed with the *rsc3^{td}* endogenous locus conversion construct. The DNA content of cells from one clone is shown. Note the presence of 4C and 8C cells, indicative of continuous endopolyploidization.

Found at doi:10.1371/journal.pgen.0030092.sg005 (69 KB PDF).

Table S1. Fertility of Diploids Generated by Mating of Various *rsc^{td}* Strains

Diploids generated by mating the indicated haploids were considered fertile (+) when over 80% of spores were able to form haploid colonies. Less than 10% of spores from a *sfh1^{td}, rsc3^{td}* diploid were able to form colonies (–). Not all combinations were generated, as indicated by NT (not tested).

Found at doi:10.1371/journal.pgen.0030092.st001 (30 KB DOC).

Table S2. Yeast Strains Employed by Campsteijn et al.

Notes: (i) All the yeast strains we generated are descendants of the W303-derived YN2 and YN18 strains and all harbor *ADE2* and the *trp1–1, ura3–1, his3–11;15, and leu2–3;112* alleles; (ii) All the degron alleles were first introduced into the YN106 diploid strain and haploid strains were obtained by sporulation; (iii) Lysine auxotrophy was not systematically verified. When a strain is Lys^- it harbors the *Δlys2::rKWD50N* allele [85].

Found at doi:10.1371/journal.pgen.0030092.st002 (96 KB DOC).

Acknowledgments

We thank Francis Stewart, Henk Stunnenberg, and the members of the Nijmegen Molecular Biology Department for stimulating discussions; H. Adams, J. F. Diffley, M. R. Gartenberg, E. Herrero, D. J. Lew, K. Nasmyth, C. L. Peterson, and N. Schilderink for providing essential strains and reagents; as well as B. Gerritsen, M. Hupkes, M. Kamp, M. Rits, and B. Vergeer for assistance during their student internships.

Author contributions. CC and CL conceived and designed the experiments, analyzed the data, contributed reagents/materials/analysis tools, and wrote the paper. All authors performed the experiments.

Funding. This work was supported by the Dutch Council for Chemical Research of the Netherlands Organization for Scientific Research (NWO-CW).

Competing interests. The authors have declared that no competing interests exist.

References

1. Makalowski W (2001) Are we polyploids? A brief history of one hypothesis. Genome Res 11: 667–670.
2. Zimmet J, Ravid K (2000) Polyploidy: Occurrence in nature, mechanisms, and significance for the megakaryocyte-platelet system. Exp Hematol 28: 3–16.
3. Edgar BA, Orr-Weaver TL (2001) Endoreplication cell cycles: More for less. Cell 105: 297–306.
4. Larkins BA, Dilkes BP, Dante RA, Coelho CM, Woo YM, et al. (2001) Investigating the hows and whys of DNA endoreduplication. J Exp Bot 52: 183–192.
5. Rice LM, Plakas C, Nickels JT Jr (2005) Loss of meiotic rereplication block in *Saccharomyces cerevisiae* cells defective in Cdc28p regulation. Eukaryotic Cell 4: 55–62.
6. Castellano MM, del Pozo JC, Ramirez-Parra E, Brown S, Gutierrez C (2001) Expression and stability of *Arabidopsis* CDC6 are associated with endoreplication. Plant Cell 13: 2671–2686.
7. Bermejo R, Vilaboa N, Cales C (2002) Regulation of CDC6, geminin, and CDT1 in human cells that undergo polyploidization. Mol Biol Cell 13: 3989–4000.
8. Melixetian M, Ballabeni A, Masiero L, Gasparini P, Zamponi R, et al. (2004) Loss of geminin induces rereplication in the presence of functional p53. J Cell Biol 165: 473–482.
9. Gonzalez MA, Tachibana KE, Adams DJ, van der Weyden L, Hemberger M, et al. (2006) Geminin is essential to prevent endoreduplication and to form pluripotent cells during mammalian development. Genes Dev 20: 1880–1884.
10. MacAuley A, Cross JC, Werb Z (1998) Reprogramming the cell cycle for endoreduplication in rodent trophoblast cells. Mol Biol Cell 9: 795–807.
11. Schild D, Ananthaswamy HN, Mortimer RK (1981) An endomitotic effect of a cell-cycle mutation of *Saccharomyces cerevisiae*. Genetics 97: 551–562.
12. Thomas JH, Botstein D (1986) A gene required for the separation of chromosomes on the spindle apparatus in yeast. Cell 44: 65–76.
13. Rose MD, Fink GR (1987) *KAR1*, a gene required for function of both intranuclear and extranuclear microtubules in yeast. Cell 48: 1047–1060.
14. Luca FC, Winey M (1998) *MOB1*, an essential yeast gene required for completion of mitosis and maintenance of ploidy. Mol Biol Cell 9: 29–46.
15. Chan CS, Botstein D (1993) Isolation and characterization of chromosome-gain and increase-in-ploidy mutants in yeast. Genetics 135: 677–691.
16. Schubeler D, Turner BM (2005) A new map for navigating the yeast epigenome. Cell 122: 489–492.
17. Clayton AL, Hazzalin CA, Mahadevan LC (2006) Enhanced histone acetylation and transcription: A dynamic perspective. Mol Cell 23: 289–296.
18. Flaus A, Owen-Hughes T (2004) Mechanisms for ATP-dependent chromatin remodeling: Farewell to the tuna-can octamer? Curr Opin Genet Dev 14: 165–173.
19. Saha A, Wittmeyer J, Cairns BR (2006) Chromatin remodeling: The industrial revolution of DNA around histones. Nat Rev Mol Cell Biol 7: 437–447.
20. Cairns BR, Lorch Y, Li Y, Zhang M, Lacomis L, et al. (1996) RSC, an essential, abundant chromatin-remodeling complex. Cell 87: 1249–1260.
21. Winston F, Carlson M (1992) Yeast SNF/SWI transcriptional activators and the SPT/SIN chromatin connection. Trends Genet 8: 387–391.
22. Peterson CL, Herskowitz I (1992) Characterization of the yeast *SWI1, SWI2,* and *SWI3* genes, which encode a global activator of transcription. Cell 68: 573–583.
23. van Vugt JJFA, Ranes M, Campsteijn C, Logie C (2007) The ins and outs of ATP-dependent chromatin remodeling: Biophysical and proteomic perspectives. Biochim Biophys Acta 1769: 153–171.
24. Mohrmann L, Verrijzer CP (2005) Composition and functional specificity of SWI2/SNF2 class chromatin remodeling complexes. Biochim Biophys Acta 1681: 59–73.
25. Tsuchiya E, Uno M, Kiguchi A, Masuoka K, Kanemori Y, et al. (1992) The *Saccharomyces cerevisiae NPS1* gene, a novel CDC gene which encodes a 160-kDa nuclear protein involved in G2 phase control. EMBO J 11: 4017–4026.
26. Du J, Nasir I, Benton BK, Kladde MP, Laurent BC (1998) Sth1p, a *Saccharomyces cerevisiae* Snf2p/Swi2p homolog, is an essential ATPase in RSC and differs from Snf/Swi in its interactions with histones and chromatin-associated proteins. Genetics 150: 987–1005.
27. Ng HH, Robert F, Young RA, Struhl K (2002) Genome-wide location and regulated recruitment of the RSC nucleosome-remodeling complex. Genes Dev 16: 806–819.
28. Damelin M, Simon I, Moy TI, Wilson B, Komili S, et al. (2002) The genome-wide localization of Rsc9, a component of the RSC chromatin-remodeling complex, changes in response to stress. Mol Cell 9: 563–573.
29. Chai B, Huang J, Cairns BR, Laurent BC (2005) Distinct roles for the RSC and Swi/Snf ATP-dependent chromatin remodelers in DNA double-strand break repair. Genes Dev 19: 1656–1661.
30. Koyama H, Itoh M, Miyahara K, Tsuchiya E (2002) Abundance of the RSC nucleosome-remodeling complex is important for the cells to tolerate DNA damage in *Saccharomyces cerevisiae*. FEBS Lett 531: 215–221.
31. Shim EY, Ma JL, Oum JH, Yanez Y, Lee SE (2005) The yeast chromatin remodeler RSC complex facilitates end- joining repair of DNA double-strand breaks. Mol Cell Biol 25: 3934–3944.
32. Huang J, Hsu JM, Laurent BC (2004) The RSC nucleosome-remodeling complex is required for Cohesin's association with chromosome arms. Mol Cell 13: 739–750.
33. Hsu JM, Huang J, Meluh PB, Laurent BC (2003) The yeast RSC chromatin-remodeling complex is required for kinetochore function in chromosome segregation. Mol Cell Biol 23: 3202–3215.
34. Tsuchiya E, Hosotani T, Miyakawa T (1998) A mutation in *NPS1/STH1,* an essential gene encoding a component of a novel chromatin-remodeling complex RSC, alters the chromatin structure of *Saccharomyces cerevisiae* centromeres. Nucleic Acids Res 26: 3286–3292.
35. Soutourina J, Bordas-Le Floch V, Gendrel G, Flores A, Ducrot C, et al. (2006) Rsc4 connects the chromatin remodeler RSC to RNA polymerases. Mol Cell Biol 26: 4920–4933.
36. Hosotani T, Koyama H, Uchino M, Miyakawa T, Tsuchiya E (2001) PKC1, a protein kinase C homologue of *Saccharomyces cerevisiae,* participates in microtubule function through the yeast EB1 homologue, BIM1. Genes Cells 6: 775–788.
37. Chai B, Hsu JM, Du J, Laurent BC (2002) Yeast RSC function is required for organization of the cellular cytoskeleton via an alternative PKC1 pathway. Genetics 161: 575–584.
38. Versteege I, Sevenet N, Lange J, Rousseau-Merck MF, Ambros P, et al. (1998) Truncating mutations of hSNF5/INI1 in aggressive pediatric cancer. Nature 394: 203–206.
39. Roberts CW, Orkin SH (2004) The SWI/SNF complex: Chromatin and cancer. Nat Rev Cancer 4: 133–142.
40. Dohmen RJ, Wu P, Varshavsky A (1994) Heat-inducible degron: A method for constructing temperature-sensitive mutants. Science 263: 1273–1276.
41. Labib K, Tercero JA, Diffley JF (2000) Uninterrupted MCM2–7 function required for DNA replication fork progression. Science 288: 1643–1647.
42. Rao H, Uhlmann F, Nasmyth K, Varshavsky A (2001) Degradation of a cohesin subunit by the N-end rule pathway is essential for chromosome stability. Nature 410: 955–959.
43. Mendenhall MD, Hodge AE (1998) Regulation of Cdc28 cyclin-dependent protein kinase activity during the cell cycle of the yeast *Saccharomyces cerevisiae*. Microbiol Mol Biol Rev 62: 1191–1243.
44. Sia RA, Herald HA, Lew DJ (1996) Cdc28 tyrosine phosphorylation and the morphogenesis checkpoint in budding yeast. Mol Biol Cell 7: 1657–1666.
45. Donaldson AD, Raghuraman MK, Friedman KL, Cross FR, Brewer BJ, et al. (1998) CLB5-dependent activation of late replication origins in *S. cerevisiae*. Mol Cell 2: 173–182.
46. Gibson DG, Aparicio JG, Hu F, Aparicio OM (2004) Diminished S-phase cyclin-dependent kinase function elicits vital Rad53-dependent checkpoint responses in *Saccharomyces cerevisiae*. Mol Cell Biol 24: 10208–10222.
47. Bueno A, Russell P (1992) Dual functions of CDC6: A yeast protein required for DNA replication also inhibits nuclear division. EMBO J 11: 2167–2176.

48. Nguyen VQ, Co C, Li JJ (2001) Cyclin-dependent kinases prevent DNA rereplication through multiple mechanisms. Nature 411: 1068–1073.
49. Piatti S, Lengauer C, Nasmyth K (1995) Cdc6 is an unstable protein whose de novo synthesis in G1 is important for the onset of S phase and for preventing a "reductional" anaphase in the budding yeast *Saccharomyces cerevisiae*. EMBO J 14: 3788–3799.
50. Segal M, Clarke DJ, Maddox P, Salmon ED, Bloom K, et al. (2000) Coordinated spindle assembly and orientation requires Clb5p-dependent kinase in budding yeast. J Cell Biol 148: 441–452.
51. Haase SB, Winey M, Reed SI (2001) Multi-step control of spindle pole body duplication by cyclin-dependent kinase. Nat Cell Biol 3: 38–42.
52. Dahmann C, Diffley JF, Nasmyth KA (1995) S-phase-promoting cyclin-dependent kinases prevent rereplication by inhibiting the transition of replication origins to a pre-replicative state. Curr Biol 5: 1257–1269.
53. Angus-Hill ML, Schlichter A, Roberts D, Erdjument-Bromage H, Tempst P, et al. (2001) A Rsc3/Rsc30 zinc cluster dimer reveals novel roles for the chromatin remodeler RSC in gene expression and cell-cycle control. Mol Cell 7: 741–751.
54. Sidorova JM, Breeden LL (2003) Rad53 checkpoint kinase phosphorylation site preference identified in the Swi6 protein of *Saccharomyces cerevisiae*. Mol Cell Biol 23: 3405–3416.
55. Sidorova JM, Breeden LL (1997) Rad53-dependent phosphorylation of Swi6 and down-regulation of CLN1 and CLN2 transcription occur in response to DNA damage in *Saccharomyces cerevisiae*. Genes Dev 11: 3032–3045.
56. Longhese MP, Foiani M, Muzi-Falconi M, Lucchini G, Plevani P (1998) DNA damage checkpoint in budding yeast. EMBO J 17: 5525–5528.
57. Cairns BR, Schlichter A, Erdjument-Bromage H, Tempst P, Kornberg RD, et al. (1999) Two functionally distinct forms of the RSC nucleosome-remodeling complex, containing essential AT hook, BAH, and bromodomains. Mol Cell 4: 715–723.
58. Visintin R, Prinz S, Amon A (1997) CDC20 and CDH1: A family of substrate-specific activators of APC-dependent proteolysis. Science 278: 460–463.
59. Surana U, Amon A, Dowzer C, McGrew J, Byers B, et al. (1993) Destruction of the CDC28/CLB mitotic kinase is not required for the metaphase to anaphase transition in budding yeast. EMBO J 12: 1969–1978.
60. Huang J, Laurent BC (2004) A role for the RSC chromatin remodeler in regulating cohesion of sister chromatid arms. Cell Cycle 3: 973–975.
61. Baetz KK, Krogan NJ, Emili A, Greenblatt J, Hieter P (2004) The ctf13-30/CTF13 genomic haploinsufficiency modifier screen identifies the yeast chromatin remodeling complex RSC, which is required for the establishment of sister chromatid cohesion. Mol Cell Biol 24: 1232–1244.
62. Taneda T, Kikuchi A (2004) Genetic analysis of RSC58, which encodes a component of a yeast chromatin remodeling complex, and interacts with the transcription factor Swi6. Mol Genet Genom 271: 479–489.
63. Schaefer JB, Breeden LL (2004) RB from a bud's eye view. Cell 117: 849–850.
64. Jorgensen P, Nishikawa JL, Breitkreutz BJ, Tyers M (2002) Systematic identification of pathways that couple cell growth and division in yeast. Science 297: 395–400.
65. Cao Y, Cairns BR, Kornberg RD, Laurent BC (1997) Sfh1p, a component of a novel chromatin-remodeling complex, is required for cell-cycle progression. Mol Cell Biol 17: 3323–3334.
66. de Bruin RA, Kalashnikova TI, Chahwan C, McDonald WH, Wohlschlegel J, et al. (2006) Constraining G1-specific transcription to late G1 phase: The MBF-associated corepressor Nrm1 acts via negative feedback. Mol Cell 23: 483–496.
67. Schwob E, Bohm T, Mendenhall MD, Nasmyth K (1994) The B-type cyclin kinase inhibitor p40SIC1 controls the G1 to S transition in *S. cerevisiae*. Cell 79: 233–244.
68. Archambault V, Ikui AE, Drapkin BJ, Cross FR (2005) Disruption of mechanisms that prevent rereplication triggers a DNA damage response. Mol Cell Biol 25: 6707–6721.
69. Archambault V, Buchler NE, Wilmes GM, Jacobson MD, Cross FR (2005) Two-faced cyclins with eyes on the targets. Cell Cycle 4: 125–130.
70. Spellman PT, Sherlock G, Zhang MQ, Iyer VR, Anders K, et al. (1998) Comprehensive identification of cell cycle-regulated genes of the yeast *Saccharomyces cerevisiae* by microarray hybridization. Mol Biol Cell 9: 3273–3297.
71. Nelson MK, Kurihara T, Silver PA (1993) Extragenic suppressors of mutations in the cytoplasmic C terminus of SEC63 define five genes in *Saccharomyces cerevisiae*. Genetics 134: 159–173.
72. Carey M, Li B, Workman JL (2006) RSC exploits histone acetylation to abrogate the nucleosomal block to RNA polymerase II elongation. Mol Cell 24: 481–487.
73. Askree SH, Yehuda T, Smolikov S, Gurevich R, Hawk J, et al. (2004) A genome-wide screen for *Saccharomyces cerevisiae* deletion mutants that affect telomere length. Proc Natl Acad Sci U S A 101: 8658–8663.
74. Gatbonton T, Imbesi M, Nelson M, Akey JM, Ruderfer DM, et al. (2006) Telomere length as a quantitative trait: Genome-wide survey and genetic mapping of telomere length-control genes in yeast. PLoS Genet 2: e35. doi:10.1371/journal.pgen.0020035
75. Verdun RE, Karlseder J (2006) The DNA damage machinery and homologous recombination pathway act consecutively to protect human telomeres. Cell 127: 709–720.
76. Vries RG, Bezrookove V, Zuijderduijn LM, Kia SK, Houweling A, et al. (2005) Cancer-associated mutations in chromatin remodeler hSNF5 promote chromosomal instability by compromising the mitotic checkpoint. Gene Dev 19: 665–670.
77. Hendricks KB, Shanahan F, Lees E (2004) Role for BRG1 in cell-cycle control and tumor suppression. Mol Cell Biol 24: 362–376.
78. Oruetxebarria I, Venturini F, Kekarainen T, Houweling A, Zuijderduijn LM, et al. (2004) P16INK4a is required for hSNF5 chromatin remodeler-induced cellular senescence in malignant rhabdoid tumor cells. J Biol Chem 279: 3807–3816.
79. Versteege I, Medjkane S, Rouillard D, Delattre O (2002) A key role of the hSNF5/INI1 tumor suppressor in the control of the G1-S transition of the cell cycle. Oncogene 21: 6403–6412.
80. Zhang ZK, Davies KP, Allen J, Zhu L, Pestell RG, et al. (2002) Cell-cycle arrest and repression of cyclin D1 transcription by INI1/hSNF5. Mol Cell Biol 22: 5975–5988.
81. Isakoff MS, Sansam CG, Tamayo P, Subramanian A, Evans JA, et al. (2005) Inactivation of the Snf5 tumor suppressor stimulates cell-cycle progression and cooperates with p53 loss in oncogenic transformation. Proc Natl Acad Sci U S A 102: 17745–17750.
82. Roberts CW, Galusha SA, McMenamin ME, Fletcher CD, Orkin SH (2000) Haploinsufficiency of Snf5 (integrase interactor 1) predisposes to malignant rhabdoid tumors in mice. Proc Natl Acad Sci U S A 97: 13796–13800.
83. Roberts CW, Leroux MM, Fleming MD, Orkin SH (2002) Highly penetrant, rapid tumorigenesis through conditional inversion of the tumor suppressor gene *Snf5*. Cancer Cell 2: 415–425.
84. Kuras L, Struhl K (1999) Binding of TBP to promoters in vivo is stimulated by activators and requires Pol II holoenzyme. Nature 399: 609–613.
85. Cheng TH, Li YC, Gartenberg MR (1998) Persistence of an alternate chromatin structure at silenced loci in the absence of silencers. Proc Natl Acad Sci U S A 95: 5521–5526.